



Available online at <http://scik.org>

J. Math. Comput. Sci. 2022, 12:38

<https://doi.org/10.28919/jmcs/6932>

ISSN: 1927-5307

## CHARACTERISTICS OF NEWTONIAN HEATING ON ELECTRICALLY CONDUCTING WATER-BASED NANO-FLUID WITH IN PERMEABLE VERTICAL MICRO-CHANNELS

MANI RAMANUJA<sup>1,2</sup>, G. GOPI KRISHNA<sup>2,\*</sup>, HARI KAMALA SREE<sup>3</sup>, S.R. MISHRA<sup>4</sup>

<sup>1</sup>Department of Mathematics, GITAM Institute of Technology and Management, Bangalore,  
Karnataka – 561203, India

<sup>2</sup>Department of Mathematics, Marri Laxman Reddy Institute of Technology & Management, Dundigal,  
Hyderabad – 500 043, India

<sup>3</sup>Department of Physics, MLR Institute of Technology, Dundigal, Hyderabad-500043, India

<sup>4</sup>Department of Mathematics, Siksha ‘O’ Anusandhan Deemed to be University,  
Bhubaneswar-751030, Odisha, India

Copyright © 2022 the author(s). This is an open access article distributed under the Creative Commons Attribution License, which permits unrestricted use, distribution, and reproduction in any medium, provided the original work is properly cited.

**Abstract:** Micro-channels are extensively used in the electrical and medical industries to advance the heat transfer of cooling devices. For the present study, the heat transfer from a porous vertical micro-channel heat sink here in this work, nanofluid, was considered a working fluid inside the micro-channel. The four most commonly used nanofluid is considered during the work, that is and. The mixture of nano-sized copper and alumina particles is considered to be cool the micro-channel heat sink. The said physical model is translated into mathematical expressions are solved the governing equations analytically. It was observed that all the nano-fluids thermophysical properties vary with the addition of nano-particles, and thermal conductivity is increasing. The consequences of solid nano-particle, porosity and heat source slip parameter, Darcy number, Hartmann number, and slip length are

---

\*Corresponding author

E-mail address: [drgopikrishnag@gmail.com](mailto:drgopikrishnag@gmail.com)

Received October 26, 2021

computed.

**Keywords:** nanofluid; porous medium; Darcy number; Hartmann number; heat source.

**2010 AMS Subject Classification:** 93A30.

## 1. INTRODUCTION

The examination of incompressible viscous nanofluid free convection processes due to the importance of their existence in diverse physical measures such as heat exchangers, petroleum reservoirs, combustion modeling, and fire engine. The flow phenomena over the micro-channel are also generating a lot of attention since they have practical implications in accumulating for electronics and computers. Researchers and scientists have persistent because nano-fluids act as a unique heat transfer medium. They can get better conductivity of the fluids by adding tiny solid nano-particles, resulting in increased heat transfer for various applications.

Tuckerman and Pease [1] first heat sink researchers introduced a method for draining heat from a chip by pushing coolant via closed channels imprinted on the underside of silicon wafer. Experimental, numerical, and theoretical investigations are the three types of studies conducted in this area. Ozoë and Okada [2] analyzed the influence of the magnetic field path in a cubical enclosure was investigated it using a three-dimensional numerical model. Oztop *et al.* [3] analyses using a finite volume approach the heat transfer and fluid flow induced by magnetohydrodynamic buoyancy in a non-isothermally heated square enclosure. The entropy created in a simple engineering system is proportionate to the energy destroyed, which is always destroyed owing to the Second Law. Koo and Kleinstreuer [4] discussed with a temperature rise, there is a more significant augmentation in thermal conductivity. Nayak *et al.* [5] analyses the influence of physical parameters on a water-based  $Al_2O_3$  nanofluid using the KKL model.

The concept of nanofluid is demonstrated experimentally by Choi *et al.*[6] and examined when compared to a simple base fluid, an increase in thermal efficiency. These findings were subsequently tested in the experiment (Kang *et al.*[7]). Further, Eastman *et al.* [8] proposed

water-based nano-fluids using copper ( $Cu$ ) and aluminium oxide ( $Al_2O_3$ ) and noticed the comparison to conventional base fluids, thermal conductivity may unquestionably boost the rate of heat transfer capacities of nanofluids. Various types of flow models, and presenting techniques and hybrid nanofluid applications, have been explored in light of the concept of thermal conductivity of nano-fluids. Aybar *et al.* [9] and Ahmed *et al.* [10] examined the composing flow dynamics are being squeezed nanoparticles  $Al_2O_3$  nanoparticles between two analogous disks. Heat transfer and skin friction's analytical and numerical effects were also highlighted.

Hayat *et al.* [11] investigated the MHD nanofluid flow across a stretched surface with power-law velocity as an analytical problem. Domairry *et al.* [12] have examined shows the thickness of the momentum bounding surface grows as the volume fraction of nanoparticles enhances, whereas the thickness of the thickness of the thermal boundary layer diminishes. Sheikholeslami *et al.* [13] have investigated a revolving system with two horizontal plates, the flow of nanofluids, and heat transfer properties; their findings show that raising the nanoparticle volume percentage and the injection/suction parameter enhances the heat transfer rate at the surface for suction/injection.

The increase in heat conductivity was proportional to the particle size, according to Esfahani and Toghraie [14] and Beck *et al.* [15], but Anoop *et al.* [16] found the reverse. Aysha *et al.* [17] found that Cu-water nanofluid showed improved thermal enhancement trends than  $Al_2O_3$ -water nanofluid when the Reynolds number was increased. Kirsch and Thol [18] and concluded micro-channel pin fin arrays were created using laser powder bed fusion and tested for pressure loss and heat transfer over a range of Reynolds numbers. Ambreen and Kim [19] examined the flow of nanofluids in the tube under laminar and turbulent conditions. They discovered that Brownian motion in nanofluids causes an enhancement in the heat coefficient near the intake.

Sun *et al.* [20] the variations of nanofluid heat transfer rate was investigated experimentally ( $Fe_3O_2$  /water) under the influence of the magnetic field within the horizontal circular tubes. They established a relation between the intensity of the magnetic field and the pace of heat transmission. Kumar *et al.* [21] evaluated heat transfer rates for conventional fluid and nanofluid

were numerically compared. ( $Al_2O_3 / H_2O$ ) claimed that nanofluid resulted in for the reduction in temperature as well as a 70% boost in the dependability of electronic chips. Lahmar *et al.* [22] examined including a squeezing flow of water, the behavior of thermal conductivity, and heat transfer rate  $Fe_3O_2 / water$  with the effect of the magnetic field within two parallel plates. Nada *et al.* [23] investigated mixed convection flow in a lid-driven inclined square enclosure filled with a nanofluid. Manoj Kumar *et al.* [24] investigated an MHD nanofluid flows and generates entropy in a vertical channel with a deformable porous medium. Younes *et al.* [25] are discussed Advances of nanofluids in heat exchangers-A review.

According to the author's knowledge and information based on the above literature, the influence of limited nanofluid particles was considered. In the present study, a comparison of vertical micro-channels with equal heat transfer areas in different conditions is suitable for heat transfer. Also, the impact of water and on the thermal performance of vertical micro-channels was considered. Considering all of the articles mentioned above, we studied the influence of the magnetic field and nanoparticles on the flow of nanofluid, which is examined by the vertical micro-channel via permeable surface with convective conditions. We studied three different types of nanofluids to investigate these effects, namely  $Al_2O_3$ -water, water and Cu-water. Various non-dimensional situations were presented and analyzed using an analytical solution, leading parameters on velocity, temperature, thermal radiation, heat source, slip parameter, Darcy number, and Hartmann number, slip length.

## 2. PHYSICAL MODEL AND GOVERNING EQUATIONS

The laminar fully developed nanofluid flow and heat transfer in a vertical micro-channel are analyzed and the results. The two plates are separated apart by a distance  $h$ . We should have used a y-axis is perpendicular to the x-axis and the x-axis is vertically upwards in the Cartesian coordinate system to the flow direction. The channel walls are at positions in which the axes' origins are  $Y = 0$  and  $Y = 1$  as seen in Fig. 1. A uniform magnetic field  $B_0$  acts normal to the

plates. The fluid is a water-based nanofluid with three different types of nano-particles in it  $Cu$  and  $Al_2O_3$ . The base fluid and incomplete nano-particles are considered to be in thermal equilibrium. Table 1 shows the thermophysical characteristics of nanofluids. In the equations of motion, temperature buoyancy forces are thought to have a linear effect on density.

Following ([26, 27 & 28]) the MHD mixed convective vertical micro-channel nanofluid flow phenomena can be expressed as;

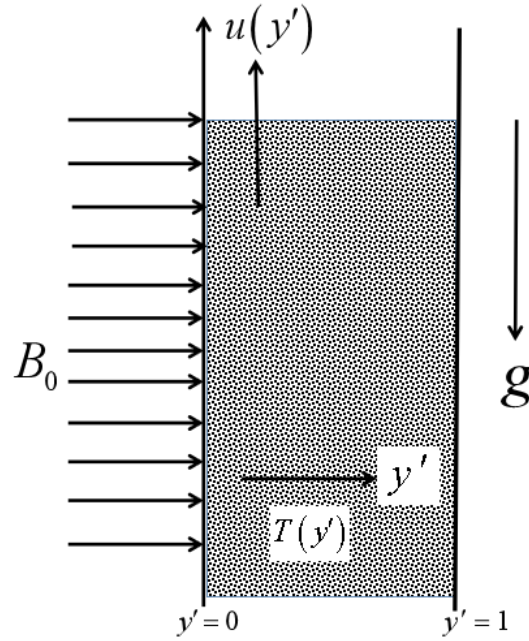


**Fig 1: Schematic Diagram**

Case I (The super-hydrophobic surface being heated-SHS)

$$\mu_{nf} \frac{d^2 u}{dy'^2} + g \rho \beta (T - T_0) - \sigma_{nf} B_0^2 u - \frac{\mu_{nf}}{K} u = 0 \quad (1)$$

$$\frac{K_{nf}}{(\rho cp)_{nf}} \frac{d^2 T}{dy'^2} - \frac{1}{(\rho cp)_{nf}} \frac{\partial q_r}{\partial y} + Q_0 = 0 \quad (2)$$

Where  $u$  is the velocity of the fluid along the  $x$ -direction,  $\rho_{nf}$  the density of the nanofluid, where  $T$ , the nanofluid temperature,  $K_{nf}$  the thermal conductivity,  $\mu_{nf}$ , the dynamic viscosity,  $\sigma_{nf}$ , the electrical conductivity, and  $(\rho cp)_{nf}$ , the heat capacitance, which is given by

$$\begin{aligned} \mu_{nf} &= \frac{\mu_f}{(1-\phi)^{2.5}}, \quad \rho_{nf} = (1-\phi)\rho_f + \phi\rho_s, \quad \sigma_{nf} = \sigma_f \left[ 1 + \frac{3(\sigma-1)}{(\sigma+2)-(\sigma-1)\phi} \right], \quad \sigma = \frac{\sigma_s}{\sigma_f}, \\ (\rho\beta)_{nf} &= (1-\phi)(\rho\beta)_f + \phi(\rho\beta)_s, \quad (\rho cp)_{nf} = (1-\phi)(\rho cp)_f + \phi(\rho cp)_s, \\ k_{nf} &= k_f \left[ \frac{k_s + 2k_f - 2\phi(k_f - k_s)}{k_s + 2k_f + \phi(k_f - k_s)} \right] \end{aligned} \quad (3)$$

The conditions of their respective boundaries are

$$\left. \begin{aligned} u(y') &= \lambda' \frac{du}{dy'} \\ T(y') &= T_h + \gamma' \frac{dT}{dy'} \end{aligned} \right\} \text{ at } y' = 0 \quad (4)$$

$$\left. \begin{aligned} u(y') &= 0 \\ T(y') &= T_0 \end{aligned} \right\} \text{ at } y' = L \quad (5)$$

Using the dimensionless similarity variables listed below

$$\begin{aligned} (Y, \gamma, \lambda) &= (y', \gamma', \lambda') / L, \quad \theta = (T - T_0) / (T_h - T_0), \quad M^2 = \sigma B_0^2 L^2 / \rho\nu, \quad \beta = \frac{Q_0 h^2}{K_0 (T_h - T_0)}, \\ U &= uv \left[ g \beta L^2 (T_h - T_0) \right]^{-1}, \quad a_4 = \left[ \frac{k_s + 2k_f - 2\phi(k_f - k_s)}{k_s + 2k_f + \phi(k_f - k_s)} \right], \quad a_1 = \frac{1}{(1-\phi)^{2.5}}, \\ a_2 &= 1 + \frac{3(\sigma-1)}{(\sigma+2)-(\sigma-1)\phi}, \quad a_3 = 1 - \phi + \phi \frac{(\rho\beta)_s}{(\rho\beta)_f} \end{aligned} \quad (6)$$

The governing equations (1) and (2) along with the boundary conditions (4) and (5) becomes

$$a_1 \frac{d^2 U}{dY^2} - M^2 a_2 U + a_3 \theta - \frac{1}{Da} a_1 U = 0 \quad (7)$$

$$(a_4 + Rd) \frac{d^2 \theta}{dY^2} + \beta = 0 \quad (8)$$

$$\left. \begin{aligned} \theta(y) &= 0 \\ U(Y) &= 0 \end{aligned} \right\} \text{ at } Y = 1 \quad (9)$$

$$\left. \begin{aligned} \theta(Y) &= 1 + \gamma \frac{d\theta}{dY} \\ U(Y) &= \lambda \frac{dU}{dY} \end{aligned} \right\} \text{ at } Y = 0 \quad (10)$$

### Case II (The no-slip surface being heated-NSS)

Solve Equations (7) and (8), using the accompanying limit conditions

$$\left. \begin{aligned} T(y') &= T_0 + \gamma' \frac{dT}{dy'} \\ u(y') &= \lambda' \frac{du}{dy'} \end{aligned} \right\} \text{ at } y' = 0 \quad (11)$$

$$\left. \begin{aligned} T(y') &= T_h \\ u(y') &= 0 \end{aligned} \right\} \text{ at } y' = L \quad (12)$$

$$\left. \begin{aligned} T(Y) &= \gamma \frac{d\theta}{dY} \\ u(Y) &= \lambda \frac{dU}{dY} \end{aligned} \right\} \text{ at } Y = 0 \quad (13)$$

$$\left. \begin{aligned} T(Y) &= 1 \\ u(Y) &= 0 \end{aligned} \right\} \text{ at } Y = 1 \quad (14)$$

**Table I**

Thermophysical properties of water and nanoparticles ([24 & 29])

Physical properties	Water/based fluid	<i>Cu</i> (Copper)	<i>Al<sub>2</sub>O<sub>3</sub></i> (Alumina)
$\rho$ (kg/m <sup>3</sup> )	997.1	8933	3970
$c_p$ (J/kg K)	4179	385	765
$k$ (w/mK)	0.613	401	40
$\sigma$ (S/m)	$5.5 \times 10^{-6}$	$59.6 \times 10^6$	$35 \times 10^6$
$\beta \times 10^5$ (K <sup>-1</sup> )	21	1.67	0.85
$\phi$	0.0	0.05	0.15

### 3. SOLUTION OF THE PROBLEM

For the coupled differential equations, analytical solutions were obtained (7 and 8) given the view of boundary conditions (9 and 10) are presented here.

#### Case I: (The super-hydrophobic surface being heated- SHS)

$$\theta = -\frac{\beta}{a_4 + Rd} \frac{y^2}{2} + C_1 y + C_2 \quad (15)$$

$$U = C_3 e^{\sqrt{d_4} y} + C_3 e^{-\sqrt{d_4} y} \left[ 1 - \frac{d_1}{d_4} y^2 + \frac{d_2}{d_4} y + \frac{d_3}{d_4} - \frac{2d_1}{d_4^2} \right] \quad (16)$$

Where  $C_1 = \frac{1}{1 + \gamma} \left[ -1 + \frac{\beta}{2(a_4 + Rd)} \right]$  ,  $C_2 = 1 + C_1 \gamma$

$$C_3 = \frac{1}{1 - \lambda \sqrt{d_4}} \left[ -C_4 (1 + \lambda \sqrt{d_4}) + \lambda \frac{d_2}{d_4} - \frac{d_3}{d_4} + 2 \frac{d_1}{d_4^2} \right]$$

$$C_4 = \frac{1}{(1 + \lambda \sqrt{d_4}) e^{\sqrt{d_4}} - (1 - \lambda \sqrt{d_4}) e^{-\sqrt{d_4}}} \left[ (1 + \lambda e^{\sqrt{d_4}}) \frac{d_2}{d_4} + (1 - e^{\sqrt{d_4}}) \frac{d_3}{d_4} + (e^{\sqrt{d_4}} - 1) \left( 2 \frac{d_1}{d_4^2} \right) - \frac{d_1}{d_4} \right]$$

$$d_1 = \frac{a_3 \beta}{2a_1(a_4 + Rd)}, d_2 = \frac{a_3}{a_1} C_1, d_3 = \frac{a_3}{a_1} C_2, d_4 = m^2 \frac{a_2}{a_1} + \frac{1}{Da}$$

#### Case II: (The no-slip surface being heated -NSS)

For the coupled differential equations, analytical solutions were obtained (7 to 8) given view of boundary conditions (13 and 14) are presented here

$$\theta = -\frac{\beta}{a_4 + Rd} \frac{y^2}{2} + C_1 y + C_2 \quad (17)$$

$$U = C_3 e^{\sqrt{d_4} y} + C_3 e^{-\sqrt{d_4} y} \left[ 1 - \frac{d_1}{d_4} y^2 + \frac{d_2}{d_4} y + \frac{d_3}{d_4} - \frac{2d_1}{d_4^2} \right] \quad (18)$$

Where  $C_1 = \frac{1}{1 + \gamma} \left[ 1 + \frac{\beta}{2(a_4 + Rd)} \right]$  ,  $C_2 = C_1 \gamma$

$$C_3 = \frac{1}{1 - \lambda \sqrt{d_4}} \left[ -C_4 (1 + \lambda \sqrt{d_4}) + \lambda \frac{d_2}{d_4} - \frac{d_3}{d_4} + 2 \frac{d_1}{d_4^2} \right]$$

$$C_4 = \frac{1}{(1 + \lambda\sqrt{d_4})e^{\sqrt{d_4}} - (1 - \lambda\sqrt{d_4})e^{-\sqrt{d_4}}} \left[ (1 + \lambda e^{\sqrt{d_4}}) \frac{d_2}{d_4} + (1 - e^{\sqrt{d_4}}) \frac{d_3}{d_4} + (e^{\sqrt{d_4}} - 1) \left( 2 \frac{d_1}{d_4^2} \right) - \frac{d_1}{d_4} \right]$$

$$d_1 = \frac{a_3 \beta}{2a_1(a_4 + Rd)}, d_2 = \frac{a_3}{a_1} C_1, d_3 = \frac{a_3}{a_1} C_2, d_4 = m^2 \frac{a_2}{a_1} + \frac{1}{Da}$$

#### 4. VOLUME FRACTION

The Volume flow rate in the vertical micro-channel, which is given by

$$Q = \int_0^1 U dY = \frac{C_3}{\sqrt{d_4}} (e^{\sqrt{d_4}} - 1) + \frac{C_4}{\sqrt{d_4}} (1 - e^{-\sqrt{d_4}}) - \frac{1}{3} \frac{d_1}{d_4} + \frac{1}{2} \frac{d_2}{d_4} + \frac{d_3}{d_4} - \frac{2d_1}{d_4^2} \quad (19)$$

#### 5. SKIN FRICTION

The Skin friction at the two vertical walls  $Y=0$  and  $Y=1$  are given by

$$\tau_{0,1} = \left( \frac{dU}{dY} \right)_{Y=0,1} \quad (20)$$

#### 6. RESULT AND DISCUSSION

We investigated the naturally convective flow and heat transmission in a viscous incompressible nanofluid (with water as the base fluid and solid nano-particles are metallic oxide-aqueous nanofluids/  $Cu$ -water and  $Al_2O_3$ -water) in this article. Nano-fluids are investigated by the vertical micro-channel. The systems of nonlinear ODE's (7 and 8) with the boundary conditions (9- 10 and 13-14) are incorporated with the analytical technique. The impact of different physical parameters insight into the flow problem, in the presence of a thermal radiation, heat source, slip parameter, Darcy number, Hartmann number, slip length, which is computed. The results are illustrated graphically, and the graphical effects are depicted in Figures (2 to 9), the red line represents pure water, the green line  $cu$ -water and the blue line represents  $Al_2O_3$ -water nanofluid. The results are performed by taking values of some constant parameters as  $M = 1, R = 1, \beta = 1, \lambda = 1, \gamma = 1$ .

Fig.2 shows the temperature profile for dissimilar nanofluid comparisons, pure water,  $Cu$

-nanofluid, and  $Al_2O_3$  nanofluid flow on radiation parameters. Fig2. Shows a comparison between pure fluid,  $Cu$ -water, and water- $Al_2O_3$ . Nanofluid decreases with an increase in the thermal radiation parameter. It is evident that nanofluid  $Cu$ -nanofluid heat transfer rate is greater than  $Al_2O_3$  nanofluid. The temperature profiles of the flow are seen to improve as the radiation parameter is increased. Physically, a rise in radiation allows heat to move, which improves to enhance momentum and the thickness of the thermal wall layer.

Supplementary, fig. 3 illustrates the impact of internal heat source parameter  $\beta$  on the temperature for pure water,  $Cu$ -Nano and  $Al_2O_3$  nanofluid. By increasing  $\beta$ , exothermic reaction generates internal heat in the thermal system, This leads to a faster of the thermal field nanofluid  $Cu$ -water- $Al_2O_3$ . It is observed that high thermal conductivity nanoparticles improve heat transmission more than low thermal conductivity nanoparticles. The influence of rising values of the heat source parameter is to enhance the temperature of nanofluid particles namely  $Cu$  water and  $Al_2O_3$  and water. The rate of transfer of heat energy on the surface can be enhanced by the addition of nanoparticles. Fig.4 shows the behaviour of velocity slip parameter  $\gamma$  on pure water,  $Cu$ -nano and  $Al_2O_3$  -nanofluid temperature. We observed an interesting effect that the profiles of nanofluid temperature, pure water,  $Cu$ -nano and  $Al_2O_3$  nanofluid increase respectively, with the decrease in velocity slip parameter  $\gamma$ . In coolants, the  $Al_2O_3$ -water nanofluid provided better heat transfer velocity as contrast to a condensed water and  $Cu$ -nanofluid. However, as compared to water, the  $Cu$ -nanofluid has a higher thermal performance.

Fig.5 represents the effect of different values of Darcy number and porosity on the pure water,  $Cu$ -nano and  $Al_2O_3$  nanofluid velocity profile. Also, the curves displaying the influence of Darcy number for  $Al_2O_3$ -water nanofluid lie connection the curves of  $Cu$ -water nanofluid,

which indicates that  $Cu$ -water nanofluid displays higher stability as a comparison to  $Cu$ -water nanofluid in the current structure.

Fig.6 corresponds to the variation of nanofluid on the velocity profile of the flow. Increasing the radiation parameter reduces the flow velocity profiles. Figure.7 illustrates the influence of Hartmann number on the main velocity, base water,  $Cu$ -nanofluid and  $Al_2O_3$  nanofluid. The velocity distribution of nanofluid clearly diminishes, with an enhance in Hartmann. This happens naturally because when the Hartmann field is enhanced, the opposing force, represented by the well-known Lorentz force, is enhanced. It is clear that the velocity of  $Al_2O_3$ -water nanofluid is more than that of  $Cu$ -water nanofluid. The base fluid, water, has lower specific gravity than both the nanofluid and the nanofluid. Fig.8 represents the impact of  $\beta$  of nanofluid on the velocity profile of the flow. The influence heat sure parameter on the nanofluid, It is clear that the comparison to  $Al_2O_3$  and  $Cu$  nanofluid due to the dominance of the conduction heat transfer mode. This is because  $Cu$  and  $Al_2O_3$  in comparison to other nanofluid particles, they exhibit the highest thermal conductivity. The  $Cu$  and  $Al_2O_3$  the heat diffusivity of nano particles is very high (compared to  $Al_2O_3$  and  $Cu$  nano) and therefore, this decreases temperature gradients, which can have an impact on performance of  $Cu$  and  $Al_2O_3$  nanoparticles. Thermal conductivity increases with large particle size.

Fig.9 represents the impact of  $\lambda$  of nanofluid on the velocity description. It is clear that the velocity of heat transfer in  $Cu$ -water nanofluid is faster than that of  $Al_2O_3$ -water nanofluid, and spherical-shaped nanoparticles in actual fact, enhances the heat transfer velocity. Thermodynamic performance of two distinct nanofluids  $Al_2O_3$  and  $Cu$  water nanofluids gives enhanced heat transfer than the base fluids water but  $Cu$ /water the MCHS has shown better thermal advantages than the water-based than the water-based  $Al_2O_3$ . Fig.10 depicts the impact

of  $\gamma$  of nanofluid on the velocity profile of the flow. In particular, the  $Al_2O_3$  nanofluid diminishes the thickness of the thermal boundary layer, which would be higher than the thickness of the  $Cu$  water solution. It shows that velocity has decreasing behaviour for large values of velocity slip parameter. It is effects for large slip parameter values;  $Cu$  \_water/nanofluid is slower than the hybrid nanofluid.

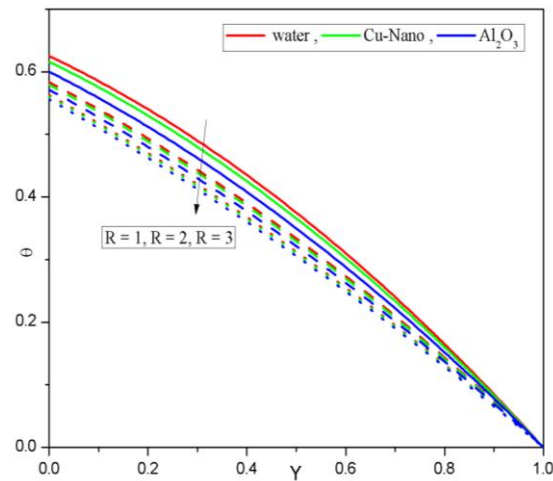


Fig.2 Impact of  $R$  of nanofluid on the temperature profile

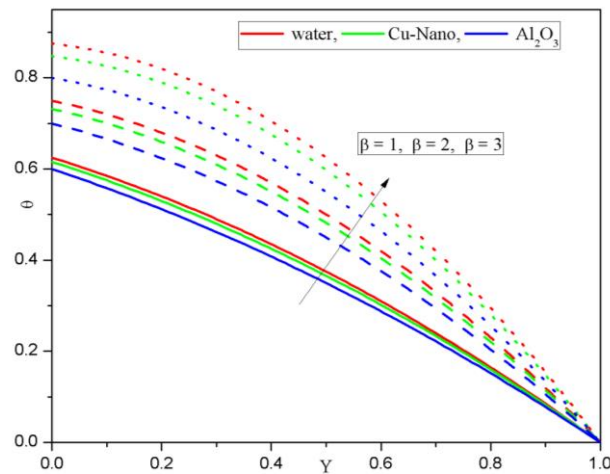
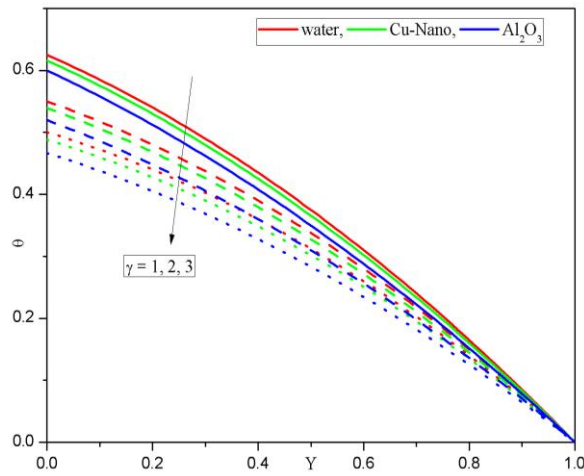
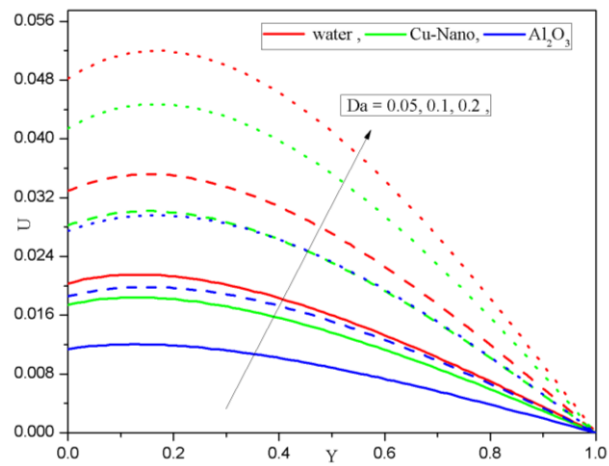
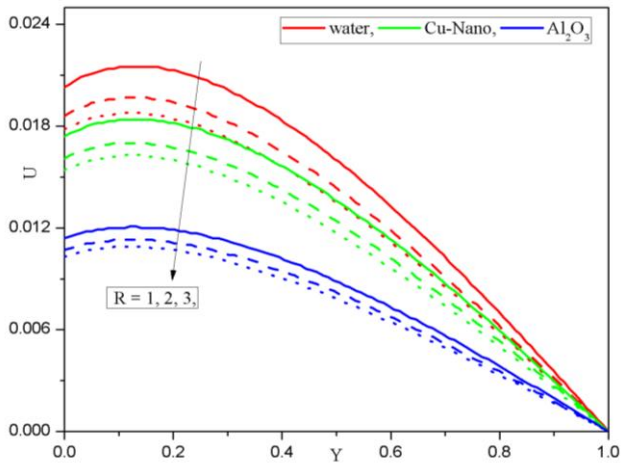
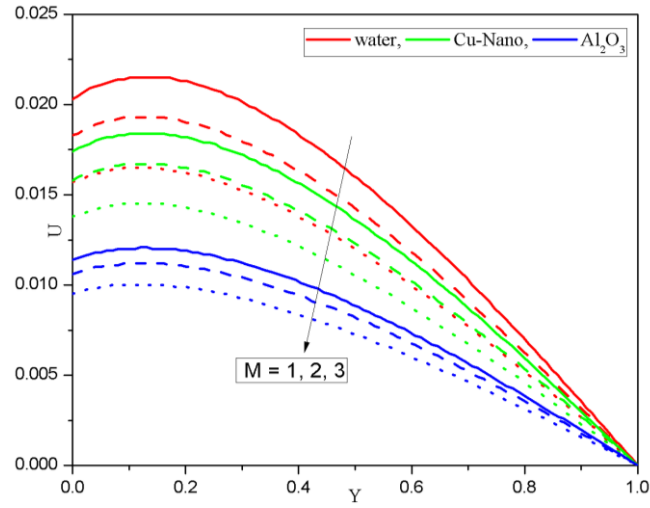
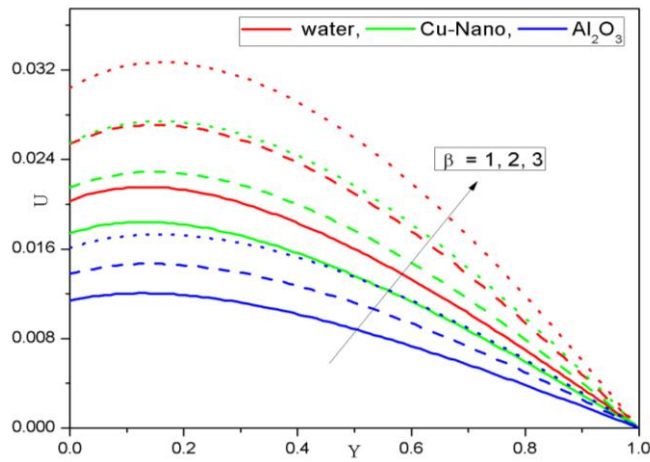
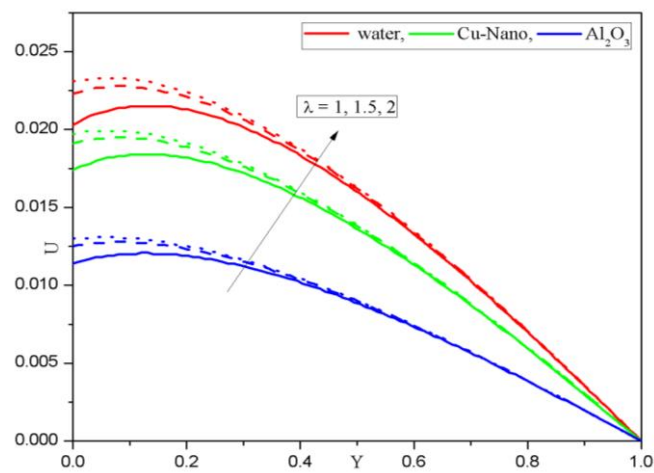


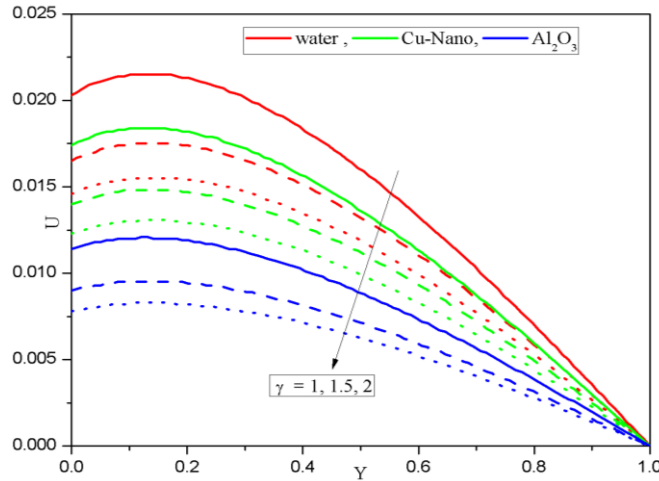
Fig.3 Impact of  $\beta$  of nanofluid on the temperature profile on temperature

## WATER-BASED NANOFLUIDS WITHIN PERMEABLE VERTICAL MICRO-CHANNELS

Fig.4 Impact of  $\gamma$  of nanofluid on the temperature profileFig.5 Impact of  $Da$  of nanofluid on the velocity profileFig.6 Impact of  $R$  of nanofluid on the velocity profile

Fig.7 Impact of  $M$  of nanofluid on the velocity profileFig.8 Impact of  $\beta$  of nanofluid on the velocity profileFig.9 Impact of  $\lambda$  of nanofluid on the velocity profile

## WATER-BASED NANOFLUIDS WITHIN PERMEABLE VERTICAL MICRO-CHANNELS

Fig.10 Impact of  $\gamma$  of nanofluid on the velocity profile**Table II** Effect of  $M$  on volume flow rate  $Q$  (Case- I)

$M$	Present work			Mani <i>et al.</i> [27], $Rd = 0$ and $\phi = 0$
	$Cu$ -Nano	$Al_2O_3$ -Nano	Pure water	Pure water
1	0.0073	0.0048	0.0085	0.0109
2	0.0058	0.0039	0.0066	0.0085
3	0.0043	0.0030	0.0048	0.0062
4	0.0031	0.0023	0.0035	0.0045

Table II shows the validation of the present analysis for the volume flow rate with the earlier work of Mani et al. [27] in case of pure fluid and the non-appearance of thermal radiation (SHS condition). Also it presents the behaviour in the case of nano-fluids. Further, it is observe that with an increase in  $M$ , the volume flow rate of nano-fluids in the vertical micro-channel decreases significantly.

**Table III** Effect of  $M$  on volume flow rate  $Q$  (Case- II)

	Present work			Mani <i>et al.</i> [27], $Rd = 0$ and $\phi = 0$
$M$	$Cu$ -Nano	$Al_2O_3$ -Nano	Pure water	Pure water
1	0.0203	0.0137	0.0234	0.0258
2	0.0156	0.0109	0.0176	0.0195
3	0.0112	0.0081	0.0125	0.0138
4	0.0081	0.0060	0.0088	0.0099

Table III illustrates the validation of the present investigation with the earlier study of [27] as well as the variation on the volume flow rate (NSS condition). In case of pure fluid both the results show their good correlation and it clarifies the convergence of the present methodology. It shows that with an increase in  $M$ , the volume flow rate of nanofluids in the vertical micro-channel decreases.

## 7. CONCLUSION

The effects of using common nano-fluids (e.g.,  $Al_2O_3/Cu/water$ ) as a effective fluid for various thermal appliances should be examined. All of the investigations explored point to nano-fluids as a viable choice for the next generation of heat transfer fluids. Analyzing the effectiveness of ( $Al_2O_3/Cu/water$ ) allows researchers to understand better the variables that influence thermo-physical properties and is highly reliant on nano-particle characteristics, temperature, and concentration. The influence of each component on  $Al_2O_3/Cu/water$  nano-fluids is shown in the following points.

- Comparative study of the current investigation concerning the earlier due to the flow of pure fluid exhibits the gateway to proceed for the further investigation with the help of metal and oxide nano-particles.

- Exothermic reaction due to the interaction of heat source leads to the strengthening of the thermal field nanofluid. However,  $Cu$ -water shows a greater rate of heat transfer than that of  $Al_2O_3$ -water nanofluid.
- The resistance of the resistive force due to the inclusion of magnetic field gives rise to Hartmann number, which results in decelerating the velocity profile within the channel.
- The influence of slip retards the thickness of the bounding surface near the channel walls of the velocity profile, whereas it favors augments the fluid temperature.

Last but not least, the current investigation and the outcomes of the result are helpful for the various recent physical phenomena like in industries as well as biomedical areas. In particular, the peristaltic flow of blood within the human body, the drug delivery process, etc. Further, the work can be extended using various nanoparticles like Carbon nanotube (CNT) of both single-wall nano-tubes (SWCNT) as well as multi-wall nanotube (MWCNT) for the enhanced properties of heat transfer.

### CONFLICT OF INTERESTS

The author(s) declare that there is no conflict of interests.

### REFERENCES

- [1] D.B. Tuckerman, R.F.W. Pease High-performance heat sinking for VLSI, IEEE Electron Device Lett. 2(5) (1981), 126–129.
- [2] H. Ozoe, K. Okada. The effect of the direction of the external magnetic field on the three-dimensional natural convection in a cubical enclosures, Int. J. Heat Mass Transfer. 32 (10) (1989), 1939-1954.
- [3] H.F. Oztop., M. Oztop., Y. Varol . Numerical simulation of magnetohydrodynamic buoyancy-induced flow in a non-isothermally heated square enclosure Commun. Nonlinear Sci. Numer. Simul. 14(3) (2009), 770-778.
- [4] J. Koo, C. Kleinstreuer, Impact analysis of nanoparticle motion mechanisms on the thermal conductivity of nanofluid, Int. Commun. Heat Mass Transf, 32(9) (2005), 1111-1118.
- [5] B. Nayak., S. R. Mishra. Analysis of the impact of physical parameters on a water-based  $Al_2O_3$  nanofluid using

- the KKL model, *Heat Transfer Res.* 50(2) (2020),1287-1307
- [6] S. Lee, S.S. Choi, S.A. Li, J.A. Eastman, Measuring thermal conductivity of fluids containing oxide nanoparticles. *J. Heat Transfer*, 121(2) (1999), 280–289.
- [7] H.U. Kang, S.H. Kim and J.M. Oh, Estimation of thermal Conductivity of nanofluid using experimental effective particle volume. *Exp. Heat Transf.* 19(3) (2006),181–191.
- [8] J.A. Eastman, S.U.S Choi, S. Li, W. Yu., L.J. Thompson. Anomalous increased effective thermal conductivities of ethylene glycol-based nanofluids containing copper nanoparticles, *Appl. Phys. Lett.* 78(6) (2001), 718–720.
- [9] H.Ş. Aybar, M. Sharifpur, M. R. Azizian, M. Mehrabi, J.P. Meyer, A review of thermal conductivity models for nanofluids. *Heat Transf. Eng.* 36(15) (2015), 1085–1110.
- [10] N. Ahmed, U. Khan, S.T. Mohyud-Din, Influence of an effective Prandtl number model on the squeezed flow of Al<sub>2</sub>O<sub>3</sub>-H<sub>2</sub>O and Al<sub>2</sub>O<sub>3</sub>-C<sub>2</sub>H<sub>6</sub>O<sub>2</sub> nanofluids, *J. Mol. Liq.* 238 (2017), 447–454.
- [11] T. Hayat., M. Rashid, M. Imtiaz, and A. Alsaedi. Magnetohydrodynamic (MHD) flow of Cu-water nanofluid due to a rotating disk with partial slip, *AIP Advances* 5(2015), 117-121.
- [12] D. Domairry, M. Sheikholeslami, H.R. Ashorynejad, R.S.R. Gorla, M. Khani, Natural convection flow of a nonnewtonian nanofluid between two vertical flat Plates, *Proc. Inst. Mech. Eng. Part N: J. Nanoeng. Nanosyst.* 225(3) (2011), 115-122.
- [13] M. Sheikholeslami, H. Ashorynejad, G. Domairry, I. Hashim, Flow and heat transfer of cu-water nanofluid between a stretching sheet and a porous surface in a rotating system, *J. Appl. Math.* 2012 (2012), 421320.
- [14] M. A. Esfahani., D.Toghraie. Experimental investigation for developing a new model for the thermal conductivity of silica/water-Ethylene glycol (40%-60%) nanofluid at different temperatures and solid volume fraction, *J. Mol. Liq.* 232 (2017), 105- 112.
- [15] M.P. Beck, Y. Yuan, P. Warriar, A.S. Teja. The thermal conductivity of alumina nanofluids in water, ethylene glycol, and ethylene glycol + water mixtures, *J. Nanopart. Res.*12(4) (2010), 1469-1477.
- [16] K.B. Anoop, T. Sundararajan, S.K. Das, Effect of particle size on the convective heat transfer in nanofluid in the developing region, *Int. J. Heat Mass Transfer.* 52 (2009), 2189–2195.
- [17] M.S. Aysha, A. Waqas, M.A. Hafiz, A. Muzaffar, A.N. Muhammad, Evaluation of nanofluids performance for

- simulated microprocessor, *Thermal Sci.* 21(5) (2017), 2227–2236.
- [18] K.L. Kirsch, K.A. Thol, Pressure loss and heat transfer performance for additively and conventionally manufactured pin fin arrays, *Int. J. Heat Mass Transf.* 108 (2017), 2502–2513.
- [19] T. Ambreen, M.H. Kim, Effect of fin shape on the thermal performance of nanofluid-cooled micro pin-fin heat sinks, *Int. J. Heat Mass Transfer*, 126 (2018), 245–256.
- [20] B. Sun, Y. Guo, D. Yang, H. Li, The Effect of constant magnetic field on convective heat transfer of Fe<sub>3</sub>O<sub>4</sub>/water magnetic nanofluid in horizontal circular tubes, *Appl. Therm. Eng.* 171 (2020), 114920.
- [21] P.M. Kumar, C.A. Kumar, Numerical study on heat transfer performance using Al<sub>2</sub>O<sub>3</sub>/water nanofluids in six circular channel heat sink for the electronic chip, *Mater. Today Proc.* 21(1) (2020), 194–201.
- [22] S. Lahmar, M. Kezzar, M.R. Eid, M.R. Sari, Heat transfer of squeezing unsteady nanofluid flow under the effects of an inclined magnetic field and variable thermal conductivity, *Phys. A Stat. Mech. Appl.* 540 (2020), 123–138.
- [23] E. Abu-Nada, A.J. Chamkha, Mixed convection flow in a lid-driven inclined square enclosure filled with a nanofluid', *Eur. J. Mech. B/Fluids*, 29(6) (2010), 472-482.
- [24] V. Manoju Kumar., S Sreenadh., G Gopi Krishna. Analysis of fluid flow and entropy generation of a MHD nanofluid through a vertical channel with deformable porous medium, *Nanosci. Technol.: Int. J.* 11(3) (2020), 223-245.
- [25] Y. Menni., Ali J Chamkha., Houari Ameer. Advances of nanofluid in heat exchangers – A review, *Heat Transfer*, 49(8) (2020),1-29.
- [26] N. Rudraiah, R.M. Barron, M. Venkatachalappa, C.K. Subbaraya, Effect of a magnetic field on free convection in a rectangular enclosure, *Int. J. Eng. Sci.* 33(8) (1995), 1075–1084.
- [27] M. Ramanuja, G.G. Krishna, H.K. Sree, V.N. Radhika, Free convection in a vertical slit micro-channel with super-hydrophobic slip and temperature jump conditions, *Int. J. Heat Technol.* 38(3) (2020), 738-744.
- [28] M.Q. Brewster, *Thermal radiative transfer and properties* Wiley, New York, 1992.
- [29] S. Das, R.N. Jana, O.D. Makinde, Mixed convective magnetohydrodynamic flow in a vertical channel filled with nanofluids, *Eng. Sci. Technol., Int. J.* 18(2) (2015), 244–255.